ORIGINAL RESEARCH

# Windkessel Measures Derived From Pressure Waveforms Only: The Framingham Heart Study

Vira Behnam, BS, BME; Jian Rong, PhD; Martin G. Larson, SD; John D. Gotal, MS; Emelia J. Benjamin, MD, ScM; Naomi M. Hamburg, MD, MS; Ramachandran S. Vasan, MD; Gary F. Mitchell, MD

***Background*—**Waveform parameters derived from pressure-only Windkessel models are related to cardiovascular disease risk and could be useful for understanding arterial system function. However, prior reports varied in their adjustment for potential confounders.

***Methods and Results*—**Carotid tonometry waveform data from 2539 participants (mean age 63±11 years, 58% women) of the Framingham Heart Study were used to derive Windkessel measures using pressure and assuming a linear model with fixed diastolic time constant ($\tau_{dias}$) and variable asymptotic pressure ($P_{inf}$, median 54.5; 25th, 75th percentiles: 38.4, 64.9 mm Hg) or nonlinear model with inverse pressure-dependent $\tau_{dias}$ and fixed $P_{inf}$ (20 mm Hg). During follow-up (median 15.1 years), 459 (18%) participants had a first cardiovascular disease event. In proportional hazards models adjusted for age, sex, total cholesterol, high-density lipoprotein cholesterol, smoking, antihypertensive medication use, diabetes mellitus, and physician-acquired systolic blood pressure, only the systolic time constant ($\tau_{sys}$) derived from the nonlinear model was related to risk for cardiovascular disease events (hazard ratio=0.91 per 1 SD, 95% CI=0.84–0.99, *P*=0.04). When heart rate was added to the model, $\tau_{sys}$ (hazard ratio=0.92, CI=0.84–1.00, *P*=0.04) and reservoir pressure amplitude (hazard ratio=1.14, CI=1.01–1.28, *P*=0.04) were related to events. In contrast, measures derived from the linear model were not related to events in models that adjusted for risk factors including systolic blood pressure (*P*>0.31) and heart rate (*P*>0.19).

***Conclusions*—**Our results suggest that pressure-only Windkessel measures derived by using a nonlinear model may provide incremental risk stratification, although associations were modest and further validation is required. **(*J Am Heart Assoc*. 2019;8: e012300. DOI: 10.1161/JAHA.119.012300.)**

**Key Words:** arterial stiffness • pressure waveform analysis • risk assessment • tau • Windkessel

Reduced models of the arterial system offer the potential to elucidate underlying mechanisms of adverse effects of vascular dysfunction. By using pressure and flow[1] waveforms or pressure alone,[2–5] modeling parameters have been derived that may predict risk for various cardiovascular disease (CVD) events.[6,7] One proposed model is based on a 3-element reservoir-wave (Windkessel) circuit,[8] consisting of a proximal series resistance, analogous to characteristic impedance, and a distal resistor and capacitor in parallel (an integrator), representing peripheral resistance ($R_p$) and total arterial compliance ($C_p$), respectively. Reservoir pressure represents the pressure attributable to the interaction of $C_p$ and accumulated change in volume (inflow−outflow) of the arterial system throughout the cardiac cycle. The remaining excess pressure component is attributed to waves produced by left ventricular ejection. The model often includes an optimized asymptotic pressure ($P_{inf}$), defined as the pressure at which arterial outflow stops, analogous to critical closing pressure.[9]

The pressure-only approach to waveform analysis is appealing because of easier implementation of cardiac risk assessment in a clinical setting. Various groups have reported different relations of this pressure-only method with clinical

*From Cardiovascular Engineering, Inc., Norwood, MA (V.B., J.D.G., G.F.M.); Boston University and NHLBI's Framingham Study, Framingham, MA (J.R., M.G.L., E.J.B., R.S.V.); Department of Biostatistics, Boston University School of Public Health, Boston, MA (M.G.L.); Cardiology and Preventive Medicine Sections, Department of Medicine (E.J.B., R.S.V.), Department of Epidemiology (E.J.B., R.S.V.), Evans Department of Medicine (N.M.H., R.S.V.), and Whitaker Cardiovascular Institute (N.M.H., R.S.V.), Boston University School of Medicine, Boston, MA.*

Accompanying Tables S1 through S4 and Figure S1 are available at https://www.ahajournals.org/doi/suppl/10.1161/JAHA.119.012300

**Correspondence to:** Gary F. Mitchell, MD, Cardiovascular Engineering, Inc., 1 Edgewater Dr, Suite 201, Norwood, MA 02062. E-mail: garyfmitchell22@gmail.com

Received April 25, 2019; accepted June 11, 2019.

## Clinical Perspective

### What Is New?

- This study examined relations between Windkessel parameters and first cardiovascular disease events in a model that accounts for standard risk factors, including heart rate and systolic blood pressure.
- The Windkessel model was modified to account for nonlinear pressure-dependence of compliance or resistance in order to better fit measured carotid waveforms without the need for a nonphysiologic asymptotic pressure ($P_{inf}$).

### What Are the Clinical Implications?

- Windkessel parameters derived from a nonlinear model were related to incident cardiovascular disease events.
- A model that explains physiological vascular parameters, such as systolic and diastolic time constants, excess and reservoir wave amplitude and $P_{inf}$, from readily accessible peripheral artery waveforms may be useful for point-of-care stratification of cardiovascular disease risk.

outcomes using different model assumptions, limited sample sizes, and variable adjustment for routinely assessed potential confounders, such as heart rate and systolic blood pressure (SBP).[2–5] In addition, several studies used peripheral (radial) arterial pressure waveforms, with or without mathematical transformations, as surrogates for central aortic pressure.[2,4,10] Directly measured carotid pressure waveforms may provide a closer substitute for central aortic pressure than those from other locations such as the radial artery.

In many of the foregoing studies, optimized values for $P_{inf}$ were much higher than physiologic values for critical closing pressure.[11] High $P_{inf}$ values may be required to optimize the fit of the linear Windkessel model because of the distinctly concave shape of the mid-to-late diastolic pressure waveform, which is not well fitted by a simple monoexponential decay. Suboptimal fitting of a concave diastolic contour may be caused by failure of the linear model to account for nonlinearity of arterial stiffness and pressure-dependence of the time constant of diastolic pressure decay, $\tau_{dias}$, which is assumed constant and equal to the product of $R_p$ and $C_p$ in a linear model.[12,13]

The goals of this analysis were 2-fold. First, we examined relations of $P_{inf}$ with pressure-dependence of $\tau_{dias}$[8,12,13] in order to elucidate requirements for nonphysiologically high values for $P_{inf}$ in previously reported studies.[14] Next, we examined independent prognostic value of hemodynamic measures derived from a pressure-only Windkessel-wave analysis of central waveforms in a community-based sample using models that adjust for standard risk factors and other confounders such as heart rate.

## Methods

The data that support the findings of this study are available from the corresponding author upon reasonable request.

## Sample

The sample includes Framingham Heart Study participants who had tonometry and relevant covariates assessed at the Original cohort 26th examination (N=304) and Offspring cohort seventh examination (N=2661). Study design criteria were described previously.[15,16] Participants with unanalyzable carotid or brachial waveforms (N=192, of whom 13 were Original cohort and 179 Offspring cohort) or prior CVD (N=234 of whom 62 were Original cohort and 172 Offspring cohort) were excluded from these analyses, resulting in the final sample (N=2539). The Boston University Medical Campus Institutional Review Board approved all study protocols, and participants provided written informed consent before participating in the study.

## Noninvasive Hemodynamics

Blood pressure and arterial tonometry of the brachial, radial, femoral, and carotid arteries were obtained in the Framingham cohorts as described previously.[17] Once acquired, data were transferred to the Core Hemodynamics Laboratory (Cardiovascular Engineering, Inc, Norwood, MA), where analyses were done without knowledge of participant characteristics. Carotid tonometry recordings were used for the present waveform analysis. The tonometry waveforms were signal averaged using the simultaneously acquired electrocardiographic R-wave as the fiducial point.[17] The brachial waveform was calibrated using SBP and diastolic blood pressure values measured at the beginning of the study by using an oscillometric device (Dinamap, GE Critikon, Milwaukee, WI). The carotid waveforms were then calibrated by using diastolic blood pressure and integrated brachial mean arterial pressure. The calibrated carotid pressure waveform was used as a surrogate for central pressure.[18]

## Waveform Modeling

Pressure waveforms were analyzed by using a segmental optimization approach.[19] First, the diastolic pressure contour was fitted by using a Nelder-Mead error minimization algorithm.[19] The systolic portion of the waveform was then optimized by finding a ratio ($\tau_{ratio}$) of diastolic ($\tau_{dias}$) to systolic ($\tau_{sys}$) tau that resulted in continuity at the dicrotic notch. For the linear model, $\tau_{dias}$ was optimized as a constant, pressure-independent value by using the following relation:

$$P(t) = (P_0 - P_{inf})\, e^{\frac{-t}{\tau_{dias}}} + P_{inf} \quad (1)$$

where P(t) is the pressure waveform at time t, $P_0$ is the optimized first point of the diastolic pressure fit at the end of systole ($T_{es}$), and $P_{inf}$ was either optimized or assumed constant (20 mm Hg). In order to avoid artifacts associated with the pre-ejection period, the end of the diastolic optimization window ($T_{ed}$) was set to a point that was 1/12th of the diastolic period before the foot of the next cardiac cycle. If optimized, the values for $P_{inf}$ were initialized to 20 mm Hg and constrained to fall between 0 mm Hg and 95% of end diastolic pressure ($P_{ed}$), which was the pressure at $T_{ed}$.

Liu et al reported that experimentally determined pressure-volume data of human aortic arch segments are nonlinear and are well fitted by exponential, logarithmic, and quadratic functions of pressure.[20] Therefore, $\tau_{dias}$ for the nonlinear tau model was calculated by assuming a mixed linear and natural logarithmic pressure-volume relation, which was differentiated in order to derive a hyperbolic relation between pressure-dependent tau, $\tau(P)$, and pressure as follows:

$$\tau(P) = \frac{m}{P} + b \quad (2)$$

where m is the slope and b is the y-intercept of the $\tau(P)$ versus 1/P relation. The variables (m, b) in Equation 2 were optimized by using the Nelder-Mead algorithm. Before optimization, initial values for m and b were estimated by performing linear regression of observed $\tau(t)$ versus 1/P(t) relations during diastole ($T_{es}$ to $T_{ed}$), where $\tau(t)=P(t)/(dP(t)/dt)$ and dP(t)/dt was obtained by direct differentiation of the pressure waveform. Points with extreme values for $\tau(t)$ (<0.2 or >20 s), which were attributable to noise in dP(t)/dt, were removed from the $\tau(t)$ and P(t) arrays before fitting. Optimized values for m and b were used to calculate reservoir pressure. The value for tau at mean arterial pressure was calculated for the nonlinear tau model and compared with fixed $\tau_{dias}$ derived from the linear model.

For linear and nonlinear methods, the systolic component of the reservoir pressure was derived by adjusting $\tau_{ratio}$ in order to achieve continuity with fitted diastolic pressure at the dicrotic notch ($P_0$). The equation that was used for reservoir pressure for the full cardiac cycle is:

$$pRes[i] = pRes[i-1] + \left[ \left( p[i] - pRes[i-1] \right) \times \frac{\tau_{ratio}}{\tau_{dias}} - \left( pRes[i-1] - P_{inf} \right) \times \frac{1}{\tau_{dias}} \right] \times \Delta t \quad (3)$$

where pRes is the reservoir pressure, i is the sample number, and $\Delta t$ is the sample time interval. The portion of the equation to the left of the minus sign in the square brackets represents inflow and the portion to the right represents outflow. The value for $\tau_{dias}$ in Equation 3 is either constant (linear model) or a function of the optimized slope and intercept of the tau-pressure relation (Equation 2). The value for $\tau_{sys}$ was then calculated from $\tau_{ratio}$ and either the fixed or variable $\tau_{dias}$. The value for $\tau_{ratio}$ was optimized by finding the first minimum in error, where error was defined as the single point difference between $P_{res}$ at $T_{es}$ and the first point of the fitted diastolic pressure curve ($P_0$).[19] Note that the variable, $\tau_{ratio}=\tau_{dias}/\tau_{sys}=(R_p \times C)/(Z_c \times C)=R_p/Z_c$ represents the ratio of total peripheral resistance ($R_p$) to characteristic impedance of the aorta ($Z_c$). Based on observations in the Framingham Offspring at a subsequent examination, when central aortic pressure and flow were measured, the upper limit for $\tau_{ratio}$ was set to the maximum value for the observed ratio, $R_p/Z_c=22$.[21] Finally, the excess pressure waveform was calculated by subtracting reservoir pressure from measured pressure at each timepoint.

For the linear model, parameters were fitted with allowance for an optimized variable $P_{inf}$, which had a lower bound at 0 mm Hg and an upper bound at 95% of end-diastolic pressure. Linear models were also done with a fixed $P_{inf}$ of 20 mm Hg, which is consistent with values for critical closing pressures that have been reported in the literature.[11,14] Waveform amplitudes were calculated as maximum pressure−pressure at the waveform foot. Waveform integrals were defined as area under the pressure-time curve, not including area below the foot of the waveform. Figure 1 depicts a sample waveform with reservoir and excess pressure waveforms derived by using a nonlinear model. Figure S1 illustrates differences in Windkessel fits and diastolic concavity for linear models with variable and fixed $P_{inf}$. We created a diastolic concavity index (DCI) as a measure of the degree of concavity of the measured and fitted curves. DCI was calculated as follows:

$$DCI = \frac{\text{Area of crescent}}{\text{Area of reference triangle}} \quad (4)$$

The reference triangle was formed using the 3 points ($T_{es}$, $P_{es}$), ($T_{ed}$, $P_{ed}$), and ($T_{es}$, $P_{ed}$), where $T_{es}$ and $P_{es}$ are the time and pressure at the start of diastole and $T_{ed}$ and $P_{ed}$ are the time and pressure at the end of diastole, respectively. The crescent is the area bounded by the exponential fit of the nonlinear model and the hypotenuse of the reference triangle. Crescent areas that fall below the hypotenuse represent positive concavity.

We tested 3 models: pressure-dependent $\tau(P)$ with fixed $P_{inf}$, constant $\tau_{dias}$ with fixed $P_{inf}$, and constant $\tau_{dias}$ with variable $P_{inf}$. The first 2 models were used to determine the similarity of derived Windkessel variables from our proposed nonlinear model and the established linear model when $P_{inf}$ was held constant. $P_{inf}$ was fixed in order to determine

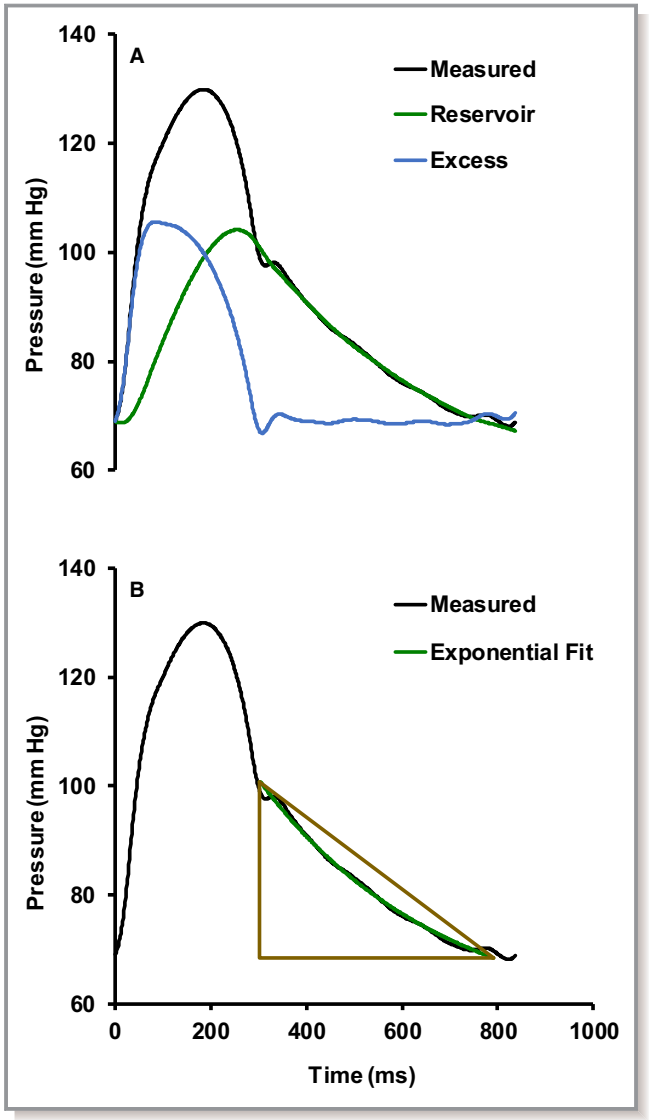


**Figure 1.** A sample pressure waveform with derived measures for the nonlinear model with fixed asymptotic pressure ($P_{inf}$). **A**, The measured waveform with reservoir and excess pressures. **B**, Illustration of diastole fit with the corresponding diastolic concavity index triangle.

whether the models can reach an optimal fit by altering other variables within a physiological range instead of setting $P_{inf}$ to an unrealistically large value. The last 2 models were used to examine the effects of variable $P_{inf}$ on other Windkessel variables in a linear model.

## Outcomes

Major CVD events include fatal and nonfatal myocardial infarction, prolonged coronary insufficiency with ECG changes, heart failure, or stroke as previously reported.[17] CVD events were identified by using medical records of hospitalizations and physician visits during follow-up. These data were reviewed by 3 investigators for event classification. Follow-up of participants extended through December 31, 2015.

## Statistical Methods

Baseline characteristics of the sample were tabulated and presented as mean±SD unless otherwise noted. Windkessel measures were tabulated and, since all were skewed, results were presented as median (25th, 75th percentiles). For analyses, all Windkessel variables were transformed using the natural logarithm. Relations between nonlinear (pressure-dependent) and linear (pressure-independent) models were evaluated using Pearson correlations. Relations between sample characteristics and Windkessel variables derived from the nonlinear model were evaluated using partial correlations adjusted for age and sex.

In order to examine the contribution of $P_{inf}$ to diastolic concavity of the linear compliance model, we examined relations of DCI of the fitted waveform with the pressure difference ($P_{diff}$) at end-diastole between the pressure waveform and asymptotic pressure (ie, $P_{diff}=P_{ed}-P_{inf}$). These analyses were performed separately for linear models with fixed and variable $P_{inf}$. We hypothesized that smaller $P_{diff}$ would be associated with greater concavity of the fitted diastolic pressure waveform.

Covariates for primary outcome analyses were selected based on prior studies and included heart rate (beats/min) as well as components of the Framingham Risk Score: age (years), sex (M/F), total cholesterol (mg/dL), high-density lipoprotein cholesterol (mg/dL), current smoking (Y/N), antihypertensive treatment (Y/N), diabetes mellitus (Y/N), and physician-acquired (clinic) SBP (mm Hg).[22] We examined associations between Windkessel variables and time to a first major CVD event using Cox proportional hazards regression models, after confirming that the assumption of proportionality was met. Covariates in Model 0 included age and sex only. Model 1 added total cholesterol, high-density lipoprotein cholesterol, smoking, antihypertensive medication use, and diabetes mellitus to Model 0. Clinic SBP was added in Model 2 and heart rate in Model 3. Windkessel variables were examined individually in the 4 sequential models. We used Model 3 to examine interactions with age, sex, and hypertension treatment for each of the Windkessel measures. All statistical analyses were done in SAS version 9.4. A 2-sided $P<0.05$ was considered significant.

# Results

## Characteristics of the Sample

After applying study inclusion criteria, we analyzed 2539 participants with mean age 63±11 years and 58% women.

Baseline characteristics of the sample are presented in Table 1. Central hemodynamic measures and results for the variable tau Windkessel-wave model are presented in Table 2. During follow-up (median 15.1 years), 459 (18%) participants had a first major CVD event (125 myocardial infarction, 11 coronary insufficiency, 168 heart failure, 125 stroke, and 30 CVD death).

## Comparison of Linear and Nonlinear Model Fits With Fixed or Variable $P_{inf}$

Descriptive statistics for Windkessel variables derived using linear and nonlinear models are presented in Table S1. Values for $\tau_{dias}$, $\tau_{sys}$, and $\tau_{ratio}$ were lower in the linear model with variable $P_{inf}$. DCI values for the linear model with fixed $P_{inf}$ were lower and had a more constrained range than values from the variable $P_{inf}$ and nonlinear models (median of 0.08 vs 0.20 and 0.18, respectively).

Relations of DCI with $P_{diff}$ (the pressure difference between $P_{ed}$ and $P_{inf}$) for linear models with fixed or variable $P_{inf}$ are presented in Figure 2. In the linear model with fixed $P_{inf}$, the range of DCI values was relatively constrained, initial diastolic error was relatively high (Table S1), and correlation between inverse DCI and $P_{diff}$ was moderate ($r^2$=0.27, Figure 2A). In the linear model with variable $P_{inf}$, values for $P_{inf}$ were high (median=54.5, first quartile=38.4, third quartile=64.9), values for DCI were higher and more broadly distributed, initial diastolic errors were lower (Table S1), and the relation between DCI and $P_{diff}$ was hyperbolic; many cases had low values for $P_{diff}$, indicating that $P_{inf}$ was at or near the upper bound (95% of $P_{ed}$). Inverse DCI with $P_{diff}$ was linear with a high degree of correlation ($r^2$=0.86, Figure 2B).

Relations between measured and optimized DCI values are presented in Figure 3. In the linear model with fixed $P_{inf}$, correlation between measured and optimized pressure waveform DCI was modest ($r^2$=0.17, Figure 3A). In the linear model with variable $P_{inf}$, correlation between measured and optimized DCI improved dramatically ($r^2$=0.75, Figure 3B). In the nonlinear model with fixed $P_{inf}$, there was a strong correlation between measured and optimized pressure waveform DCI ($r^2$=0.78, Figure 3C), despite the low value for $P_{inf}$. The foregoing results are consistent with the hypothesis that, in a linear model, a relatively high value for $P_{inf}$ (low $P_{diff}$) is

**Table 1.** Baseline Characteristics of the Sample (N=2539)

| Variable | Value |
|---|---|
| Age, y | 63±11 |
| Women, n (%) | 1472 (58) |
| Height, cm | 167±10 |
| Weight, kg | 77±17 |
| Body mass index, kg/m$^2$ | 27.7±5.1 |
| Clinic blood pressure, mm Hg | |
| Systolic | 129±20 |
| Diastolic | 74±10 |
| Pulse pressure | 55±18 |
| Heart rate, beats/min | 65±11 |
| Total cholesterol, mg/dL | 201±36 |
| HDL cholesterol, mg/dL | 55±17 |
| Hypertension treatment, n (%) | 861 (34) |
| Diabetes mellitus, n (%) | 249 (10) |
| Smoker, n (%) | 327 (13) |

Values represent mean±SD or number of samples (percentage of total). HDL indicates high-density lipoprotein.

**Table 2.** Hemodynamic Variables Derived From Carotid Pressure Waveforms Using a Nonlinear Model and Fixed Asymptotic Pressure

| Variable | Value |
|---|---|
| Central hemodynamic measures | |
| Peak systolic pressure, mm Hg | 121 (109, 134) |
| End systolic pressure, mm Hg | 99 (91, 109) |
| Diastolic pressure, mm Hg | 70 (62, 77) |
| Pulse pressure, mm Hg | 50 (41, 63) |
| Mean arterial pressure, mm Hg | 91 (84, 100) |
| Windkessel variables | |
| Diastolic tau, s | 1.1 (0.8, 1.4) |
| Systolic tau, s | 0.10 (0.08, 0.12) |
| Tau ratio, unitless | 11.2 (7.9, 15.7) |
| Reservoir pressure amplitude, mm Hg | 34.6 (27.9, 43.9) |
| Excess pressure amplitude, mm Hg | 29.2 (23.4, 37.0) |
| Excess pressure integral, mm Hg×s | 5.3 (4.0, 7.1) |
| Slope of diastolic tau-pressure relation, mm Hg×s | 138 (45, 253) |
| Intercept of diastolic tau-pressure relation, s | −0.5 (−1.6, 0.4) |
| Diastolic concavity index pressure, unitless | 0.14 (0.06, 0.21) |
| Diastolic concavity index fitted pressure, unitless | 0.18 (0.12, 0.24) |
| Diastolic error | |
| Initial diastolic root mean squared error, mm Hg | 0.9 (0.7, 1.2) |
| Single point difference at end-systole, mm Hg | 0.003 (0.001, 0.008) |
| Final diastolic root mean squared error, mm Hg | 0.8 (0.6, 1.0) |

Values represent median (25th, 75th percentiles). The diastolic and systolic time constants represent the value at mean arterial pressure.

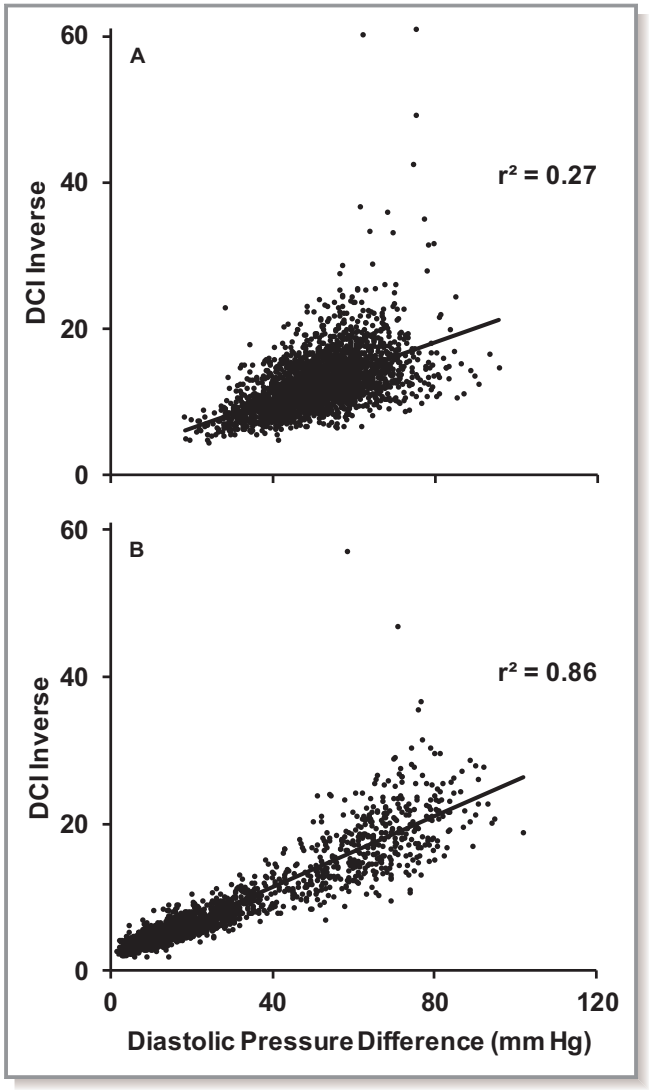


**Figure 2.** Relations between model diastolic concavity index (DCI) and diastolic pressure difference for the linear model when asymptotic pressure ($P_{inf}$) is fixed at 20 mm Hg (**A**) or optimized (**B**). Note the much wider range of values for DCI and diastolic pressure difference and the dramatic shift to a lower pressure difference and lower inverse DCI (higher concavity) in (**B**).

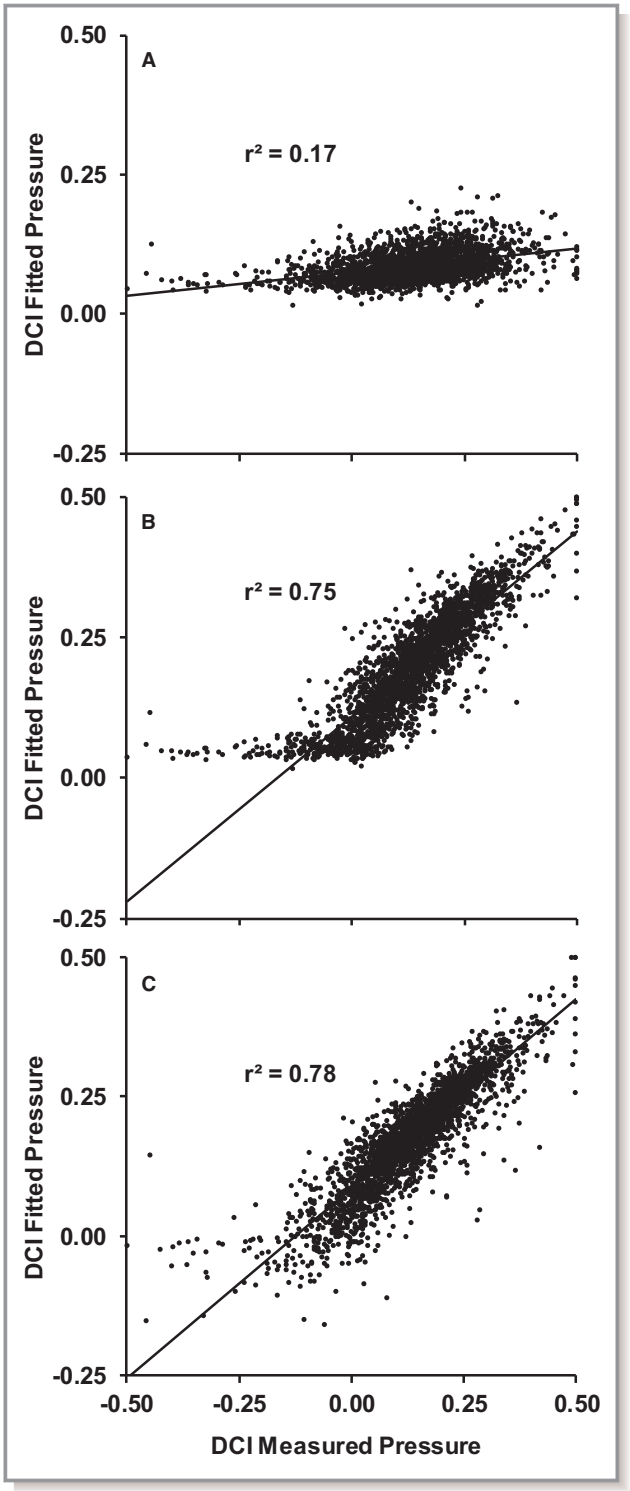


**Figure 3.** Relations between diastolic concavity index (DCI) of the fitted and measured pressures. **A**, Representation of a linear model with fixed asymptotic pressure ($P_{inf}$). **B**, The linear model with variable $P_{inf}$. **C**, The nonlinear model with fixed $P_{inf}$.

required in order to match model and measured DCI and minimize diastolic error.

Partial correlation coefficients adjusted for age and sex for the comparison of nonlinear model results versus linear models with fixed or optimized $P_{inf}$ are presented in Table S2. Correlations for $\tau_{dias}$, $\tau_{sys}$, and $\tau_{ratio}$ varied considerably. In contrast, amplitudes of pressure waveform components, including reservoir pressure amplitude, excess pressure amplitude, and excess pressure integral, were relatively highly correlated ($r$=0.81–0.97) across all models.

Partial correlation coefficients adjusted for age and sex of Windkessel variables, derived by using the nonlinear model, with various CVD risk factors, including clinic blood pressure and components of central blood pressure, are presented in Table S3. $\tau_{dias}$ correlated moderately with age, female sex, pulse pressure, and diastolic pressure decay ($P_{es}-P_{ed}$). $\tau_{ratio}$

**Table 3.** Carotid Waveform Analysis Components as Predictors of CVD Events (n=456 Incident Events)

| | Model 0 | | Model 1 | | Model 2 | | Model 3 | |
|---|---|---|---|---|---|---|---|---|
| Variable | Hazard Ratio (LCL, UCL) | *P* Value | Hazard Ratio (LCL, UCL) | *P* Value | Hazard Ratio (LCL, UCL) | *P* Value | Hazard Ratio (LCL, UCL) | *P* Value |
| Diastolic time constant, s | 0.85 (0.77, 0.95) | <0.005 | 0.87 (0.78, 0.97) | 0.01 | 0.91 (0.81, 1.01) | 0.09 | 0.95 (0.85, 1.07) | 0.38 |
| Systolic time constant, s | 0.93 (0.85, 1.02) | 0.11 | 0.90 (0.83, 0.98) | 0.02 | 0.91 (0.84, 0.99) | 0.04 | 0.92 (0.84, 1.00) | 0.04 |
| Tau ratio, unitless | 0.96 (0.87, 1.06) | 0.41 | 1.01 (0.91, 1.12) | 0.89 | 1.03 (0.93, 1.14) | 0.56 | 1.07 (0.96, 1.18) | 0.23 |
| Reservoir pressure amplitude, mm Hg | 1.11 (1.01, 1.22) | 0.04 | 1.12 (1.01, 1.24) | 0.03 | 1.05 (0.94, 1.17) | 0.41 | 1.14 (1.01, 1.28) | 0.04 |
| Excess pressure amplitude, mm Hg | 1.15 (1.04, 1.27) | 0.01 | 1.08 (0.97, 1.19) | 0.15 | 1.01 (0.90, 1.12) | 0.93 | 1.00 (0.90, 1.12) | 0.94 |
| Excess pressure integral, mm Hg×s | 1.05 (0.95, 1.15) | 0.38 | 1.00 (0.91, 1.11) | 0.97 | 0.94 (0.85, 1.04) | 0.22 | 0.97 (0.87, 1.07) | 0.52 |

Hemodynamic variables are entered individually in separate models. Model 0 is adjusted for age and sex. Model 1 is adjusted for age, sex, total cholesterol, high-density lipoprotein cholesterol, smoking, antihypertensive medication use, and diabetes mellitus. Model 2 adds clinic systolic blood pressure to Model 1. Model 3 adds heart rate to Model 2. Hazard ratios expressed per 1 SD higher value; 456 events with median of 15.1 years of follow-up. Diastolic and systolic time constants are calculated at mean arterial pressure. CVD indicates cardiovascular disease; LCL, UCL, lower and upper limits of the 95% CI. All Windkessel variables were transformed using the natural logarithm.

correlated moderately with age, female sex, and pulse pressure. Reservoir and excess pressure variables were correlated with age, SBP, pulse pressure, diastolic pressure decay, and mean arterial pressure. All Windkessel variables except $\tau_{sys}$ correlated with central pulse pressure. Reservoir pressure amplitude was highly correlated with the diastolic pressure decay, suggesting that peak reservoir pressure is approximately equal to $P_{es}$ (Figure 1).

## Relations of Windkessel Variables With Incident CVD Events

Relations of carotid Windkessel measures derived using the nonlinear model with CVD events are presented in Table 3. In Model 0, $\tau_{dias}$, reservoir pressure amplitude, and excess pressure amplitude were associated with events. In Model 1, $\tau_{dias}$, $\tau_{sys}$, and reservoir pressure amplitude were associated with events. After further adjustment for SBP (Model 2), only $\tau_{sys}$ remained associated with events. When heart rate was added (Model 3), $\tau_{sys}$ and reservoir pressure amplitude were associated with events. Interactions with age, sex, and hypertension treatment produced $P>0.05$, indicating no significant effect modification. Cox proportional hazards models for linear models with fixed or variable $P_{inf}$ are presented in Table S4. In base Model 0 with adjustments for age and sex only, excess pressure amplitude and integral were associated with events. In Model 1, only excess pressure amplitude remained associated with events. When SBP (Model 2) and then heart rate (Model 3) were added, none of the Windkessel variables were associated with events.

# Discussion

## Relations of Windkessel Variables With Incident CVD Events

In our community-based sample, in models adjusted for standard risk factors, including clinic SBP and heart rate, $\tau_{sys}$ and reservoir pressure amplitude were nominally related to events when our fit was based on the nonlinear model with fixed $P_{inf}$. In a traditional linear model with constant $\tau_{dias}$ and monoexponential pressure decay, Windkessel variables were not independently related to events in our community-based sample.

Previous studies examined the prognostic value of Windkessel variables derived from a linear pressure-only analysis. In the Kinmen Study and Cardiovascular Disease Risk Factors Community Study cohorts, Cheng et al concluded that systolic and diastolic time constants of the reservoir wave were associated with excess CVD risk.[2] In the Conduit Artery Function Evaluation study, Davies et al determined that excess pressure integral was related to events.[4] However, these studies did not account for heart rate as a potential confounder of Windkessel variables. In our linear model (Table S4), we have shown that excess pressure variables were related to events in an age- and sex-adjusted model, but after adjustment for standard risk factors, SBP and heart rate, none of those relations remained significant.

Other studies have adjusted for established risk factors and found persistent relations between Windkessel measures and CVD events in selected patient samples. Narayan et al examined a cohort of elderly, hypertensive patients and concluded that $\tau_{sys}$ was associated with risk.[3] While their

analyses accounted for standard risk factors, the study had lower precision than our study because of the small number of events in their study. Hametner et al found that the amplitude of the reservoir wave remained significant in a model that adjusted for standard CVD risk factors.[5] However, observations in their high-risk patient sample with suspected coronary artery disease cannot be generalized for risk assessment in the community. While our linear model analysis does not find any of the Windkessel variables to be related to events, our analysis for the nonlinear model with fixed $P_{inf}$ aligns with outcomes of these studies. It is also worth noting that blood pressure values of our cohort are lower on average than other populations in this age group.

The use of radial waveforms in the aforementioned articles (except for Narayan et al, who used carotid waveforms as in this article) could contribute to the discrepancy in excess pressure and $\tau_{sys}$ associations with our results in Table S4 (the linear tau method, fitting waveform parameters with the established Windkessel equations). However, $\tau_{dias}$ and reservoir pressure results should be the same based on the definition of a Windkessel model.

## Relevance of Asymptotic Pressure

A monoexponential pressure decay in diastole, as predicted by a linear Windkessel model, does not fit many pressure waveforms adequately. Within the physiologic pressure range for diastole (ie, starting at an end-systolic pressure of ≈110 mm Hg and falling to ≈70 mm Hg), a simple monoexponential decay appears remarkably linear, whereas diastolic pressure contours generally are distinctly concave, particularly in older people. We hypothesized that this concavity may be because of nonlinear characteristics of the arterial system representing pressure dependency of compliance, resistance, or both. In a nonlinear model, $\tau_{dias}$ varies continuously with pressure throughout the cardiac cycle.[4,12] For example, using the mean values for $\tau_{dias}$ slope and intercept and end-systolic and diastolic pressures, one can estimate that $\tau_{dias}$ increased by ≈50% between the onset and end of diastole in our sample. The resulting increase in $\tau_{dias}$ as pressure falls increases concavity of the diastolic pressure contour and eliminates the need for high $P_{inf}$ values in order to fit the diastolic pressure contour. An alternative interpretation of a high degree of concavity of a monoexponential decay is that the asymptotic pressure is near the minimum pressure (ie, that $P_{inf}$ is near diastolic pressure). In the latter case, the slope of the waveform will rapidly approach zero as diastolic pressure approaches $P_{inf}$. However, direct measurements of pressure during prolonged asystole have shown that the pressure waveform decays to values that are well below diastolic blood pressure.[10]

Figure 2 demonstrates the effect of $P_{inf}$ on the concavity of the waveform, as measured by DCI. There is a modest relation between the inverse of DCI and diastolic pressure difference ($P_{diff}$) when $P_{inf}$ is fixed. DCI is severely restricted in this model, even for visually concave waveforms, and the diastolic pressure difference reaches a floor value at ≈20 mm Hg. When the same variables are plotted for the variable $P_{inf}$ case, the relation is hyperbolic and DCI spans a wider range of values. When the inverse of DCI is plotted against the diastolic pressure difference, a strong linear relation is observed. Our observations indicate that high values for $P_{inf}$ in the linear model may help to match the concavity of measured and modeled pressures by serving as a surrogate for pressure dependence of compliance or resistance.

An important consequence of using variable $P_{inf}$ to optimize waveform fit is the effect on other optimized variables. As shown in Table S1, when $P_{inf}$ was optimized, the resulting $\tau_{dias}$ was reduced by ≈50% as compared with models with fixed $P_{inf}$. As a result, the optimized $\tau_{ratio}$ is also lower. In Table S2, low correlations between values for $\tau_{dias}$, $\tau_{sys}$, and $\tau_{ratio}$ in the fixed and variable $P_{inf}$ models demonstrate that $P_{inf}$ variably alters these time-based waveform characteristics. Therefore, consideration of the pressure dependence of tau may be required in order to accurately characterize other Windkessel parameters. However, reservoir and excess pressure amplitudes were similar and highly correlated for linear and nonlinear models, suggesting that the approach to waveform fitting has only a modest effect on the amplitudes of these pressure waveform components.

This study has limitations that need to be considered. The Framingham Heart Study cohorts examined in this report consist of participants who are predominantly white and older, so these results may not be generalizable to younger age groups or different races and ethnicities. It is worth noting that blood pressure values of this cohort are lower on average than other populations in this age group. This study was observational; therefore, a causal effect cannot be determined for any of the Windkessel variables tested. This study assumes carotid artery measurements are a substitute for the central aorta. This study also assumes the pressure-volume relation of the arterial system is logarithmic, but there may be other models that represent the physiological relations more accurately. It is worth noting that noninvasive cuff measurements of diastolic blood pressure have been shown to be, on average, 5.5 mm Hg above intra-arterial values[23]; therefore, true tau and $P_{inf}$ values may deviate from the calculated values in this article.

In summary, our findings indicate that pressure dependence of tau needs to be incorporated into the reservoir-wave model in order to produce realistic optimized Windkessel parameters to describe the arterial system. With the foregoing refinement, we were able to demonstrate that Windkessel measures derived from pressure alone may provide

independent CVD risk discrimination after accounting for standard risk factors and heart rate. We have previously shown that measures derived from pressure and flow (forward pressure wave amplitude) but not pressure alone (primary pressure wave amplitude) were predictive of events in models that included standard risk factors.[24] Future studies should examine the relevance of Windkessel model parameters when results are derived from measured pressure and flow.

## Sources of Funding

This work was supported by the National Heart, Lung, and Blood Institute's Framingham Heart Study (contracts N01-HC-25195 and HHSN268201500001I) and NIH grants HL126136, HL107385, HL070100, and HL060040. Dr Vasan is supported in part by the Evans Medical Foundation and the Jay and Louis Coffman Endowment from the Boston University School of Medicine.

## Disclosures

Dr Mitchell is the president of Cardiovascular Engineering, Inc, a company that designs and manufactures devices that measure vascular stiffness, and serves as a consultant to and receives honoraria and grant support from Novartis, Servier, Merck, and the National Institutes of Health. V. Behnam and J. Gotal are employees of Cardiovascular Engineering, Inc. The remaining authors have no disclosures to report.

## References

1. Wang JJ, O'Brien AB, Shrive NG, Parker KH, Tyberg JV. Time-domain representation of ventricular-arterial coupling as a Windkessel and wave system. *Am J Physiol Heart Circ Physiol*. 2003;284:H1358–H1368.
2. Cheng HM, Chuang SY, Wang JJ, Shih YT, Wang HN, Huang CJ, Huang JT, Sung SH, Lakatta EG, Yin FC, Chou P, Yeh CJ, Bai CH, Pan WH, Chen CH. Prognostic significance of mechanical biomarkers derived from pulse wave analysis for predicting long-term cardiovascular mortality in two population-based cohorts. *Int J Cardiol*. 2016;215:388–395.
3. Narayan O, Davies JE, Hughes AD, Dart AM, Parker KH, Reid C, Cameron JD. Central aortic reservoir-wave analysis improves prediction of cardiovascular events in elderly hypertensives. *Hypertension*. 2015;65:629–635.
4. Davies JE, Lacy P, Tillin T, Collier D, Cruickshank JK, Francis DP, Malaweera A, Mayet J, Stanton A, Williams B, Parker KH, McG Thom SA, Hughes AD. Excess pressure integral predicts cardiovascular events independent of other risk factors in the conduit artery functional evaluation substudy of Anglo-Scandinavian Cardiac Outcomes Trial. *Hypertension*. 2014;64:60–68.
5. Hametner B, Wassertheurer S, Hughes AD, Parker KH, Weber T, Eber B. Reservoir and excess pressures predict cardiovascular events in high-risk patients. *Int J Cardiol*. 2014;171:31–36.
6. Segers P, Rietzschel ER, De Buyzere ML, Stergiopulos N, Westerhof N, Van Bortel LM, Gillebert T, Verdonck PR. Three- and four-element Windkessel models: assessment of their fitting performance in a large cohort of healthy middle-aged individuals. *Proc Inst Mech Eng H*. 2008;222:417–428.
7. Shim Y, Pasipoularides A, Straley CA, Hampton TG, Soto PF, Owen CH, Davis JW, Glower DD. Arterial Windkessel parameter estimation: a new time-domain method. *Ann Biomed Eng*. 1994;22:66–77.
8. Sagawa K, Lie RK, Schaefer J. Translation of Otto Frank's paper "Die Grundform des Arteriellen Pulses" Zeitschrift fur Biologie 37: 483-526 (1899). *J Mol Cell Cardiol*. 1990;22:253–254.
9. Shrier I, Hussain SN, Magder S. Effect of carotid sinus stimulation on resistance and critical closing pressure of the canine hindlimb. *Am J Physiol*. 1993;264:H1560–H1566.
10. Chirinos JA, Kips JG, Jacobs DR Jr, Brumback L, Duprez DA, Kronmal R, Bluemke DA, Townsend RR, Vermeersch S, Segers P. Arterial wave reflections and incident cardiovascular events and heart failure: MESA (Multiethnic Study of Atherosclerosis). *J Am Coll Cardiol*. 2012;60:2170–2177.
11. Kottenberg-Assenmacher E, Aleksic I, Eckholt M, Lehmann N, Peters J. Critical closing pressure as the arterial downstream pressure with the heart beating and during circulatory arrest. *Anesthesiology*. 2009;110:370–379.
12. Alastruey J. On the mechanics underlying the reservoir-excess separation in systemic arteries and their implications for pulse wave analysis. *Cardiovasc Eng*. 2010;10:176–189.
13. Langewouters GJ, Wesseling KH, Goedhard WJ. The static elastic properties of 45 human thoracic and 20 abdominal aortas in vitro and the parameters of a new model. *J Biomech*. 1984;17:425–435.
14. Chemla D, Lau EMT, Herve P, Millasseau S, Brahimi M, Zhu K, Sattler C, Garcia G, Attal P, Nitenberg A. Influence of critical closing pressure on systemic vascular resistance and total arterial compliance: a clinical invasive study. *Arch Cardiovasc Dis*. 2017;110:659–666.
15. Dawber TR, Kannel WB. The Framingham Study. An epidemiological approach to coronary heart disease. *Circulation*. 1966;34:553–555.
16. Kannel WB, Feinleib M, McNamara PM, Garrison RJ, Castelli WP. An investigation of coronary heart disease in families. The Framingham Offspring Study. *Am J Epidemiol*. 1979;110:281–290.
17. Mitchell GF, Hwang SJ, Vasan RS, Larson MG, Pencina MJ, Hamburg NM, Vita JA, Levy D, Benjamin EJ. Arterial stiffness and cardiovascular events: the Framingham Heart Study. *Circulation*. 2010;121:505–511.
18. Kelly R, Fitchett D. Noninvasive determination of aortic input impedance and external left ventricular power output: a validation and repeatability study of a new technique. *J Am Coll Cardiol*. 1992;20:952–963.
19. Aguado-Sierra J, Alastruey J, Wang JJ, Hadjiloizou N, Davies J, Parker KH. Separation of the reservoir and wave pressure and velocity from measurements at an arbitrary location in arteries. *Proc Inst Mech Eng H*. 2008;222:403–416.
20. Liu Z, Brin KP, Yin FC. Estimation of total arterial compliance: an improved method and evaluation of current methods. *Am J Physiol*. 1986;251:H588–H600.
21. Mitchell GF, Wang N, Palmisano JN, Larson MG, Hamburg NM, Vita JA, Levy D, Benjamin EJ, Vasan RS. Hemodynamic correlates of blood pressure across the adult age spectrum: noninvasive evaluation in the Framingham Heart Study. *Circulation*. 2010;122:1379–1386.
22. D'Agostino RB Sr, Vasan RS, Pencina MJ, Wolf PA, Cobain M, Massaro JM, Kannel WB. General cardiovascular risk profile for use in primary care: the Framingham Heart Study. *Circulation*. 2008;117:743–753.
23. Picone DS, Schultz MG, Otahal P, Aakhus S, Al-Jumaily AM, Black JA, Bos WJ, Chambers JB, Chen CH, Cheng HM, Cremer A, Davies JE, Dwyer N, Gould BA, Hughes AD, Lacy PS, Laugesen E, Liang F, Melamed R, Muecke S, Ohte N, Okada S, Omboni S, Ott C, Peng X, Pereira T, Pucci G, Rajani R, Roberts-Thomson P, Rossen NB, Sueta D, Sinha MD, Schmieder RE, Smulyan H, Srikanth VK, Stewart R, Stouffer GA, Takazawa K, Wang J, Westerhof BE, Weber F, Weber T, Williams B, Yamada H, Yamamoto E, Sharman JE. Accuracy of cuff-measured blood pressure: systematic reviews and meta-analyses. *J Am Coll Cardiol*. 2017;70:572–586.
24. Cooper LL, Rong J, Benjamin EJ, Larson MG, Levy D, Vita JA, Hamburg NM, Vasan RS, Mitchell GF. Components of hemodynamic load and cardiovascular events: the Framingham Heart Study. *Circulation*. 2015;131:354–361.

# SUPPLEMENTAL MATERIAL

**Table S1. Windkessel measures derived from carotid pressure waveforms by using a nonlinear model with fixed asymptotic pressure or a linear model with fixed or variable asymptotic pressure.**

| | Nonlinear Fixed $P_{inf}$ | Linear Fixed $P_{inf}$ | Linear Variable $P_{inf}$ |
|---|---|---|---|
| Diastolic tau, s | 1.1 (0.8, 1.4) | 1.2 (1.0, 1.5) | 0.49 (0.37, 0.76) |
| Systolic tau, s | 0.10 (0.08, 0.12) | 0.13 (0.11, 0.16) | 0.09 (0.07, 0.11) |
| Tau ratio, unitless | 11.2 (7.9, 15.7) | 9.1 (6.6, 12.4) | 6.0 (4.0, 9.4) |
| Reservoir pressure amplitude, mm Hg | 34.6 (27.9, 43.9) | 30.7 (25.4, 37.0) | 34.2 (27.9, 42.3) |
| Excess pressure amplitude, mm Hg | 29.2 (23.4, 37.0) | 30.5 (24.3, 39.3) | 26.4 (21.0, 33.5) |
| Excess pressure integral, mm Hg x s | 5.3 (4.0, 7.1) | 6.3 (4.7, 8.6) | 5.0 (3.7, 6.7) |
| Diastolic concavity index fitted pressure, unitless | 0.18 (0.12, 0.24) | 0.08 (0.07, 0.10) | 0.20 (0.13, 0.26) |
| Initial diastolic root mean squared error, mm Hg | 0.9 (0.7, 1.2) | 1.3 (0.9, 1.7) | 0.8 (0.6, 1.1) |
| Single point difference at end-systole, mm Hg | 0.003 (0.001, 0.008) | 0.003 (0.001, 0.007) | 0.004 (0.001, 0.009) |
| Final diastolic root mean error, mm Hg | 0.8 (0.6, 1.0) | 1.1 (0.8, 1.5) | 0.7 (0.5, 0.9) |

Values represent median ($25^{th}$, $75^{th}$ percentiles). For nonlinear models, diastolic and systolic time constants are calculated at mean arterial pressure. $P_{inf}$ is the diastolic asymptotic pressure. For variable carotid $P_{inf}$ model, $P_{inf}$ was 54.5 (38.4, 64.9). All other models had a fixed $P_{inf}$ of 20 mm Hg.

**Table S2. Pearson correlation coefficients adjusted for age and sex comparing linear and nonlinear models.**

| | Model $P_{inf}$ | |
|---|---|---|
| **Variable** | **Fixed** | **Variable** |
| Diastolic tau, s | 0.90 | 0.43 |
| Systolic tau, s | 0.43 | 0.82 |
| Tau ratio, unitless | 0.77 | 0.46 |
| Reservoir pressure amplitude, mm Hg | 0.90 | 0.97 |
| Excess pressure amplitude, mm Hg | 0.95 | 0.94 |
| Excess pressure integral, mm Hg x s | 0.81 | 0.90 |

Each column represents results from a constant tau model, without and with variable asymptotic pressure ($P_{inf}$) compared to a reference nonlinear model with fixed asymptotic pressure of 20 mm Hg. For the nonlinear model, the diastolic and systolic time constants were calculated at mean arterial pressure. Correlation coefficients with an absolute value greater than 0.066 are significant at $P<0.001$. All Windkessel variables were transformed using the natural logarithm.

**Table S3. Partial correlations adjusted for age and sex of various risk factors relations with Windkessel measures derived by using a nonlinear model with fixed asymptotic pressure.**

| | Diastolic Tau, s* | Systolic Tau, s* | Tau Ratio, unitless | Reservoir Pressure Amp, mm Hg | Excess Pressure Amp, mm Hg | Excess Pressure Integral, mm Hg x s |
|---|---|---|---|---|---|---|
| Age, y† | -0.42 | -0.02 | -0.33 | 0.37 | 0.43 | 0.38 |
| Women‡ | -0.42 | 0.05 | -0.39 | 0.12 | 0.12 | 0.24 |
| Height, cm | 0.10 | 0.12 | -0.03 | -0.07 | 0.03 | 0.04 |
| Weight, kg | -0.03 | 0.16 | -0.17 | -0.02 | 0.22 | 0.16 |
| Body mass index, kg/m$^2$ | -0.08 | 0.12 | -0.16 | 0.01 | 0.22 | 0.15 |
| Clinic blood pressure, mm Hg | | | | | | |
| Systolic | -0.25 | -0.07 | -0.13 | 0.42 | 0.44 | 0.37 |
| Diastolic | -0.00 | -0.10 | 0.09 | 0.15 | 0.10 | 0.07 |
| Pulse pressure | -0.32 | -0.02 | -0.23 | 0.43 | 0.49 | 0.42 |
| Central pressures, mm Hg | | | | | | |
| Pulse pressure | -0.65 | -0.06 | -0.45 | 0.84 | 0.82 | 0.74 |
| Diastolic pressure decay | -0.51 | -0.29 | -0.14 | 0.90 | 0.56 | 0.51 |
| Mean arterial pressure | -0.09 | -0.09 | 0.02 | 0.42 | 0.40 | 0.35 |

**Table S3 (continued).**

| | Diastolic Tau, s* | Systolic Tau, s* | Tau Ratio, unitless | Reservoir Pressure Amp, mm Hg | Excess Pressure Amp, mm Hg | Excess Pressure Integral, mm Hg x s |
|---|---|---|---|---|---|---|
| Heart rate, beats/ min | -0.23 | 0.06 | -0.24 | -0.26 | 0.07 | -0.06 |
| Total cholesterol, mg/dL | -0.01 | -0.04 | 0.03 | 0.02 | 0.01 | 0.00 |
| HDL cholesterol, mg/dL | 0.00 | -0.04 | 0.04 | 0.01 | -0.07 | -0.03 |
| Hypertension treatment | -0.02 | 0.02 | -0.04 | 0.11 | 0.14 | 0.12 |
| Diabetes mellitus | -0.07 | 0.07 | -0.12 | -0.00 | 0.13 | 0.08 |
| Smoker | -0.03 | -0.02 | -0.00 | -0.03 | -0.04 | -0.03 |

Values represent Pearson partial correlation coefficients adjusted for age and sex. Tau, time constant; Amp, amplitude. All Windkessel variables were transformed using the natural logarithm. Correlation coefficients with an absolute value greater than 0.066 are significant at P<0.001. *Calculated at mean arterial pressure. †Adjusted for sex. ‡Adjusted for age.

**Table S4. Relations with CVD events of various carotid waveform components derived by using a linear model with variable asymptotic pressure.**

| | Model 0 | | Model 1 | | Model 2 | | Model 3 | |
|---|---|---|---|---|---|---|---|---|
| Variable | Hazard Ratio (LCL, UCL) | P | Hazard Ratio (LCL, UCL) | P | Hazard Ratio (LCL, UCL) | P | Hazard Ratio (LCL, UCL) | P |
| Diastolic time constant, s | 0.94 (0.84, 1.06) | 0.34 | 0.96 (0.85, 1.08) | 0.49 | 1.01 (0.89, 1.14) | 0.89 | 0.99 (0.88, 1.12) | 0.90 |
| Systolic time constant, s | 1.05 (0.95, 1.16) | 0.35 | 0.99 (0.90, 1.09) | 0.80 | 0.99 (0.90, 1.09) | 0.79 | 0.99 (0.90, 1.09) | 0.85 |
| Tau ratio, unitless | 0.90 (0.80, 1.02) | 0.10 | 0.97 (0.86, 1.09) | 0.64 | 1.02 (0.91, 1.15) | 0.73 | 1.00 (0.89, 1.13) | 0.97 |
| Reservoir pressure amplitude, mm Hg | 1.07 (0.97, 1.18) | 0.16 | 1.09 (0.98, 1.20) | 0.10 | 1.01 (0.91, 1.13) | 0.82 | 1.08 (0.96, 1.21) | 0.19 |
| Excess pressure amplitude, mm Hg | 1.20 (1.08, 1.33) | 0.00 | 1.12 (1.01, 1.24) | 0.03 | 1.06 (0.95, 1.19) | 0.31 | 1.05 (0.94, 1.17) | 0.43 |
| Excess pressure integral, mm Hg x s | 1.14 (1.03, 1.27) | 0.01 | 1.08 (0.97, 1.20) | 0.15 | 1.01 (0.90, 1.14) | 0.83 | 1.05 (0.93, 1.18) | 0.42 |

Hemodynamic variables are entered individually in separate models. Model 0 is adjusted for age and sex. Model 1 is adjusted for age, sex, total cholesterol, HDL cholesterol, smoking, antihypertensive medication usage and diabetes. Model 2 adds clinic systolic blood pressure to Model 1. Model 3 adds heart rate to Model 2. Hazard ratios expressed per 1 SD higher value; 456 events with median of 15.1 years of follow-up. Diastolic and systolic time constants are calculated at mean arterial pressure. LCL, UCL, lower and upper limits of the 95% confidence intervals. All Windkessel variables were transformed using the natural logarithm.

**Figure S1. Sample pressure waveforms with corresponding derived measures for the linear tau model.**

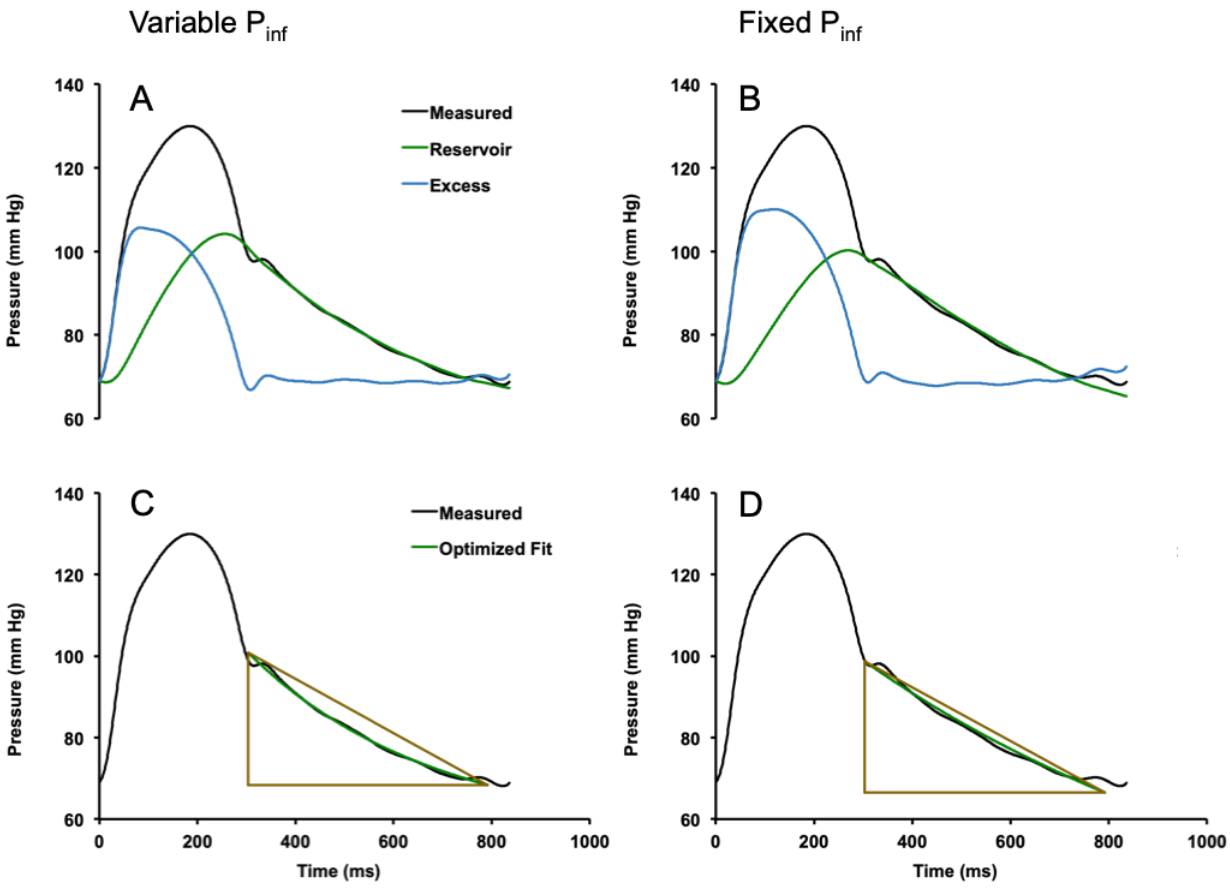


Panels A and B are the measured waveforms with reservoir and excess pressures for variable and fixed $P_{inf}$ models, respectively. Panels C and D illustrate diastole fits with corresponding diastolic concavity index triangles for variable and fixed $P_{inf}$ models, respectively.